ENHANCED CLUTTER MITIGATION IN WEATHER RADAR OBSERVATIONS THROUGH COMPARISON BETWEEN A DUAL-POLARISATION, DUAL-SCAN, AND DUAL-POLARISATION DUAL-SCAN

Ali Wardhana[1*], Rizaldi Boer[1], Bambang Dwi Dasanto[1], Danang Eko Nuryanto[2], I Putu Santikayasa[1],

[1]Geophysics and Meteorology Department, Mathematics and Science Faculty, IPB University, Jl. Raya Dramaga Kampus IPB, Babakan, Kec. Dramaga, Kabupaten Bogor, 16680

[2]Indonesian Meteorological, Climatological, and Geophysical Agency Jakarta 10620

**E-mail:* *ali.wardhana@apps.ipb.ac.id*

Received: January 5, 2026 Reviewed: February 9, 2026 Accepted: June 4, 2026

ABSTRACT

Ground clutter remains a significant source of contamination in weather radar observations, adversely affecting the interpretation of echoes and subsequent meteorological applications. This study assesses the Dual-Polarisation Dual-Scan (DPDS) framework. This Bayesian-based classifier combines polarimetric descriptors (ρ_{hv}, Z_{DR}) with temporal coherence (ρ_{12}) derived from consecutive azimuthal scans. The analysis uses I/Q data from an operational dual-polarisation C-band weather radar located in Sidoarjo, Surabaya, Indonesia. Results indicate that the DPDS framework significantly outperforms traditional Dual-Polarisation (DP) and Dual-Scan (DS) methods. For moving weather (W), the DPDS achieved a Probability of Detection (POD) of 0.939, a 313-fold improvement over the DP-only method, which suffered from severe polarimetric overlap between clutter and rain. While the clutter class exhibited a False Alarm Ratio (FAR) of 0.749, this is attributed to the 83-second scan interval of the Sidoarjo radar; over this duration, stable tropical rain remains highly correlated, mimicking the temporal signature of stationary ground clutter (C). However, the framework successfully preserved the integrity of the meteorological field, reducing the misclassification of zero-velocity weather (W_0) compared to DS-only methods and achieving an overall accuracy of 0.982. These findings highlight the effectiveness of integrating polarimetric and temporal decorrelation information to establish a more robust, physically consistent echo classification framework, particularly under challenging conditions of clutter and low-velocity weather.

Keywords: dual-polarisation radar, clutter correction, dual-scan, Bayesian classifier, weather radar

1. Introduction

Accurate and timely weather radar data play a crucial role in advancing atmospheric research and enhancing severe and high-impact weather warnings and forecasts, and have become an indispensable tool for modern meteorological services worldwide [1]. Weather radar provides critical, high-resolution, real-time data for disaster weather detection, quantitative precipitation estimation (QPE), weather forecasting, flood forecasting, severe weather monitoring, and short-term precipitation forecasting [2] - [6]. The quality and reliability of the data products derived from these systems are paramount. However, the utility of weather radar is persistently challenged by non-meteorological echoes, collectively known as clutter [7], [8].

Weather radar clutter refers to unwanted radar echoes that impede the precise detection and measurement of meteorological phenomena. Clutter can originate from diverse sources, including ground objects (such as buildings, trees, and mountains), wind turbines, and non-meteorological targets. Ground clutter can obscure meteorologically significant signals from actual weather targets, thereby impacting the accurate estimation of weather parameters such as reflectivity factor, mean velocity, and spectrum width [9]. In contrast, wind turbine clutter can saturate radar receivers, leading to erroneous estimates of wind speed, reflectivity, and rainfall rate [10]. Reflections from non-meteorological targets, such as insects, birds, dust, or other particles, can cause clear-air echoes that interfere with weather radar data [11].

The evolution of clutter mitigation in weather radar has transitioned from simple deterministic filters to complex, multi-dimensional classification frameworks. As summarised in Table 1, traditional

Table 1. Categorisation of Weather Radar Clutter Mitigation Methodologies

Methodology	Key Algorithms / Techniques	Primary Discriminants / Features
Traditional Signal Processing	Digital high-pass filters and Frequency-domain filtering [12], Adaptive clutter mitigation algorithm [13], Adaptive linear filtering [14], Clutter Mitigation Decision (CMD) [15]	Deterministic frequency analysis targeting near-zero Doppler velocity
Adaptive and Statistical Methods	Spectrum Clutter Identification (SCI) algorithm [16], [17], Adaptive Spectrum Processing (ASP) algorithm [18], Doppler filtering approaches [19], Autocorrelation spectral density [20]	Dynamic adjustment of filter parameters based on signal characteristics
Fuzzy Logic	Fuzzy logic combined with threshold discrimination [21]	Reflectivity texture (TDBZ) and Clutter Phase Alignment (CPA)
Polarimetric and Temporal	Dual-Polarisation (DP), Dual-Scan (DS), Dual Polar Dual Scan (DPDS) [22], Moving spectral depolarization ratio (MsDR) filter [23]	Co-polar correlation (ρ_{HV}), differential reflectivity (Z_{DR}), and scan-to-scan correlation (ρ_{12})
Machine Learning (ML)	Support Vector Machine (SVM), The Artificial Neural Network (ANN), The Decision Tree (DT) , Neural Network (NN) [24], [25], Gated Recurrent Unit (GRU) Neural Networks [26]	Automated feature learning from Level I I/Q time-series data

methods primarily relied on frequency-domain signal processing, such as high-pass and Doppler filtering, to isolate signals at near-zero velocity. While effective for stationary targets, these techniques often introduce a low-velocity bias by indiscriminately removing slow-moving meteorological echoes. To address these limitations, adaptive statistical and fuzzy-logic frameworks—such as the Clutter Mitigation Decision (CMD) and Spectrum Clutter Identification (SCI)—were developed to exploit single-polarisation features, including reflectivity texture and phase alignment. Dual-polarisation (DP) technology represents a breakthrough, enabling the discrimination of scatterers based on physical characteristics such as shape and consistency. However, polarimetric overlap between clutter and precipitation remains a challenge. Most recently, machine learning approaches have been employed to automate feature extraction from Level I I/Q data.

Radar systems face a fundamental conflict: increasing the maximum detectable range (Rmax) typically decreases the maximum detectable velocity (Vmax). To address this 'Doppler Dilemma,' operational scanning strategies often utilise a 'batch' strategy, alternating low and high Pulse Repetition Frequencies (PRF). While the scanning strategy manages range and velocity ambiguities, the DPDS framework acts as a post-processing classification algorithm. It processes I/Q data from consecutive dual-polarisation scans. A Bayesian classifier is then used to estimate correlation functions and separate clutter from weather signals based on physical and statistical characteristics. Bayesian classification provides a reliable quality assessment for all meteorological products, a feature increasingly sought by users of weather radar products. The availability of comprehensive and detailed classification for non-meteorological targets also facilitates a range of novel applications that utilise non-precipitation echo types and underscores the necessity of transitioning from a singular, universal quality metric for radar observations to metrics that are tailored to the application, the type of target being measured, and the specific requirements of customers [27].

Level I (In-phase/I and Quadrature/Q) data, also known as weather radar time series data, represents the raw signal generated when the radar receives an echo return. It records the signal as a complex number representing the amplitude (signal strength) and the phase, which changes from pulse to pulse due to target motion, thereby enabling Doppler velocity estimation. IQ-data is processed to obtain meteorologically significant radar "moments", which are key results used to measure, predict, and forecast various weather scenarios in weather radar operations. Most Dual-Polarisation Doppler weather radars, including ground-based polarimetric Doppler C-band (4–8 GHz) weather radar systems, produce radar moments of reflectivity (Z), mean Doppler velocity (Vr), spectrum width (σ_v), differential reflectivity (Z_{DR}), correlation coefficient (ρ_{HV}), and differential propagation phase (Φ_{DP}).

Problem Formulation. The evolution of clutter mitigation algorithms has been an iterative process aimed at addressing the limitations of previous techniques. Initially, strategies employed static clutter maps and band-stop Doppler filters to eliminate signals with near-zero velocity. However, this approach indiscriminately removed legitimate, slow-moving meteorological echoes, introducing a significant low-velocity bias [28]. To mitigate this issue, more sophisticated algorithms were developed to identify clutter before filtering. The CMD algorithm uses a fuzzy-logic framework on single-polarisation data features, such as reflectivity texture (TDBZ) and Clutter Phase Alignment (CPA). In contrast, the Spectrum Clutter Identification (SCI) algorithm leverages spectral properties. Although these advancements represent improvements, their performance is constrained by the availability of information from single-polarisation radar, which was not used in this study.

The upgrade of radar from single to Dual-Polarisation (DP) capability marked a significant breakthrough. DP variables, such as differential reflectivity (Z_{DR}) and the co-polar correlation coefficient (ρ_{hv}), describe the physical characteristics of scatterers and provide strong discrimination between uniform meteorological targets (high ρ_{hv}) and ground clutter (low ρ_{hv}) [29]. However, the primary challenge with DP-only methods lies in the "overlap" in the statistical distributions of clutter and weather variables. Certain types of ground clutter can exhibit near-zero Z_{DR} and ρ_{HV} values approaching 1.0, rendering them polarimetrically indistinguishable from some precipitation, thereby increasing the detection error rate. A separate line of research focused on the dual-scan (DS) technique, which utilises temporal correlation. Meteorological echoes decorrelate in milliseconds, whereas stationary ground clutter remains highly correlated between two consecutive scans. While this method is robust to stationary targets, it is ineffective against non-stationary clutter. Consequently, the central problem is that both DP-only and DS-only algorithms suffer from inherent ambiguities that limit their performance in complex scenarios.

Traditional methods, such as Doppler-based filters, CMD, and Dual-Polarisation thresholding, demonstrate limited robustness when dealing with clutter exhibiting partial movement, biological scattering, or mixed spectral behaviour. Dual-scan techniques mitigate this issue by exploiting temporal stability between consecutive elevation scans; however, they remain susceptible to non-stationary clutter signals. Consequently, the primary objective of this study is to enhance the discrimination between clutter and meteorological echoes in complex conditions where polarimetric and temporal characteristics overlap, without compromising crucial precipitation information. To achieve this, a classification strategy is required that utilises physically interpretable DPDS discriminants. This approach enables more reliable operational clutter mitigation for the Surabaya C-band radar system.

The Sidoarjo radar site, situated near the densely populated urban centre of Surabaya and the coast of the Madura Strait, faces distinctive clutter challenges. The presence of tall industrial structures and high-rise buildings within the Surabaya metropolitan area generates substantial stationary ground clutter, frequently obscuring developing convective cells. Additionally, the coastal topography and maritime atmospheric conditions can result in anomalous propagation (AP) echoes, which are often polarimetrically indistinguishable from precipitation when employing single-scan methodologies. These localised factors necessitate a robust mitigation framework, such as the DPDS, that integrates physical scatterer characteristics with temporal stability to ensure precise early warnings for the region's frequent coastal thunderstorms.

Supporting Theories. The limitations of DP-only and DS-only algorithms suggest a combined approach. These methods rely on independent physical principles—polarimetric properties versus temporal stability—so a combined DPDS algorithm can resolve their ambiguities. The DPDS algorithm resolves classification deadlocks through synergistic data fusion. For instance, a radar echo that is ambiguous in the polarimetric domain (e.g., clutter with ρ_{HV}~1.0 mimicking rain) can be identified as clutter in the temporal domain due to its high scan-to-scan correlation. By requiring a signal to be consistent with "weather" in both domains, the algorithm reduces false alarms and missed detections. This study uses an optimal Bayesian classifier to integrate these data sources. The classifier evaluates the conditional probability that an echo belongs to predefined classes (clutter, zero-velocity weather, or other weather) using discriminant functions from both domains, and makes a final decision based on maximum likelihood. Zero-velocity weather is considered a separate weather class due to its properties, which are predominantly similar to those of clutter signals.

Bayesian decision boundaries may be rigid in complex mixed-echo conditions with overlapping polarimetric and temporal features. To address this, a Bayesian classifier learns interactions among DPDS discriminants and radar features. It refines classification decisions by integrating the joint probability of dual-polarisation and dual-scan discriminants, thereby maximising the posterior probability and improving robustness and clutter discrimination without sacrificing meteorological information.

Research Objectives. This study aims to develop and evaluate a robust radar clutter-discrimination framework that integrates Dual-Polarisation (DP) and dual-scan (DS) information using a probabilistic Bayesian approach. The specific objectives are as follows:

1. To implement a Dual-Polarisation–Dual-scan (DPDS) framework using operational C-band weather radar data, extracting key polarimetric

(ρ_{hv}, Z_{DR}) and temporal (ρ_{12}) features to characterise meteorological and non-meteorological echoes.

2. To develop a Bayesian discriminant model that combines DP and DS features to statistically separate weather echoes, clutter, and low-motion (quasi-stationary) echoes, accounting for temporal decorrelation effects arising from scan-to-scan time separation.
3. To investigate the behaviour and limitations of dual-scan correlation (ρ_{12}) when applied to operational radar volume scans separated by tens of seconds, and to quantify its contribution to clutter discrimination when combined with polarimetric variables.
4. To evaluate and compare the classification performance of: Dual-Polarisation (DP-Only), Dual-Scan (DS-Only), and Combined DPDS approaches using standard verification metrics, including Probability of Detection (POD), False Alarm Rate (FAR), Accuracy, and overall classification accuracy.
5. To assess the robustness of the DPDS approach across different Coherent Processing Interval (CPI) lengths and Signal-to-Noise Ratio (SNR) conditions, and to analyse how temporal decorrelation and noise characteristics influence clutter–weather separability in operational radar environments.

2. Methods

Radar Data and Scan Strategy. The data used for the development and validation of the algorithm were collected by the Sidoarjo polarimetric radar site, located at latitude: 7°24'37.08" S, longitude: 112°45'37.44" E, as shown in Fig. 1.

This C-band radar is operational and has been in service since early 2025. The data are raw I/Q (In-phase and Quadrature) from two dates (October 4, 2025, and November 1, 2025). The DPDS algorithm requires a specific scanning strategy. This methodology relies on processing time-series data from two consecutive azimuthal scans performed at the same low elevation angles (0.4^0 and 1.5^0). Operational scanning strategies usually use Volume Coverage Pattern (VCP) 21, in which sequential low-level scans are often performed with different Pulse Repetition Times (PRTs) to reduce coverage and rate ambiguity. However, the DS component of the algorithm utilises VCP 88888. The radar operates at a pulse repetition frequency of 1200 Hz, with a range bin of 255 m and 496 bins (corresponding to a maximum range of approximately 126 km). The pulse width is 0.8 µs, as shown in Table 2.

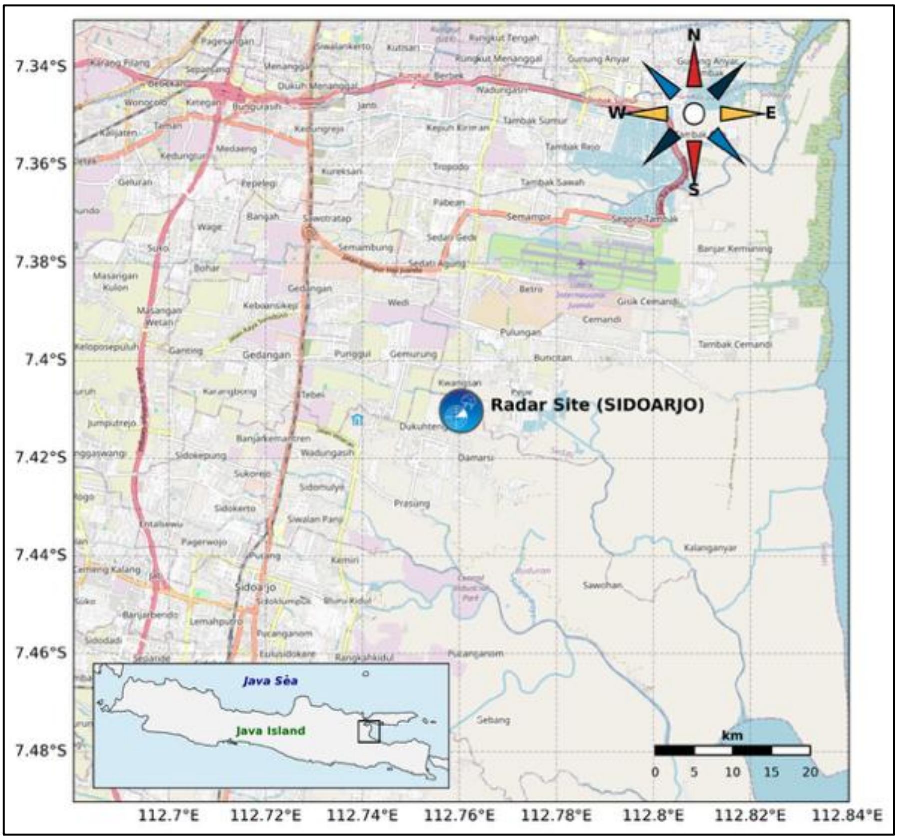

Figure 1. Radar Sidoarjo Site Location

Table 2. Waveform / Sampling Parameters

Parameter	Value
Pulse Repetition Frequency (PRF)	1200 Hz
Pulse width	0.8 µs
Gate spacing	255 m
Total gates (bins)	496
Wavelength	0.053 m (C-band)
Max range	255 * 496 ≈ 126,480 m ≈ 126 km
Maximum usable range	Limited to 2 to 30 km
Polarisation	Horizontal (H) and Vertical (V) channels were recorded independently
Elevations scanned	0.4°, 1.5° on October 4, 2025, and November 1, 2025

The Dual-Polarisation and Dual-Scan (DPDS) Algorithm. The core of the DPDS algorithm is an optimal Bayesian classifier that provides a probabilistic framework for determining clutter presence from a set of observed radar variables. A critical aspect of the algorithm's design is its use of a three-class system rather than a simple binary (clutter/no-clutter) scheme. This approach is specifically chosen to address the most challenging aspect of clutter mitigation: distinguishing stationary clutter from slow-moving or stationary weather. A binary classifier might perform well on easy cases (e.g., strong clutter vs fast-moving storms) but struggle at this ambiguous boundary. By explicitly defining and training for this challenging class, the algorithm is forced to learn the subtle statistical differences, making it inherently more robust against its most common and impactful failure mode—the erroneous filtering of legitimate low-velocity precipitation. The three classes are defined as follows:

1. Clutter (symbolised as C) is a non-meteorological echo characterized by a narrow Doppler spectrum centred at or near zero velocity.
2. Narrow-Band Zero-Velocity Weather (symbolised as W_0), a meteorological echo with properties that can resemble clutter, formally defined by thresholds such as radial velocity $|v_r| \leq 2$m/s and spectrum width $\sigma_v \leq 2$m/s. W_0 is considered a separate weather class because its properties are mostly like clutter, weak, with a mean radial velocity close to zero; thus, these weather signals commonly have longer signals and are therefore the most challenging to distinguish. Weather signals W_0 are echoes from resolution volumes where the turbulence and the mean wind radial shear are weak, with a mean radial velocity close to zero; thus, these weather signals commonly have a longer correlation time τc compared with the other weather signal (i.e., W)
3. Non-Zero-Velocity Weather (symbolised as W), all other meteorological echoes that fall outside the W_0 criteria.

W_0 are considered a separate weather class due to their properties, which are predominantly similar to those of clutter signals. The classifier calculates the probability that a given echo belongs to a clutter category (C) or a weather category (W or W_0), given a set of observed discriminant variables (X_{obs}). Given an observation of the discriminants (X_{obs}), the classifier will identify that $X = X_{obs}$ belongs to the class wi if and only if p(ωi|X_{obs}) > p (ωj|X_{obs}) for i,j Î [C, W_0, W], j > i. According to the Bayes rule, the probability of the i-th class given the observed X_{obs} can be calculated as Eq. (1):

$$P(\omega_i|X = X_{obs}) = \frac{P(X=X_{obx}|\omega i)P(\omega)}{P(X=X_{obs})} \tag{1}$$

where $P(\omega_i|X = X_{obs})$ is the posterior probability of clutter given the observations, $P(X = X_{obs}|\omega i)$is the likelihood of observing X_{obs} given that it is clutter and obtained from the statistical properties of the training data, *P(w)* is the prior probability of clutter, and $P(X=X_{obs})$ is a probability of the observations, a normalising constant. A priori probabilities are assumed to be equal for all classes, $p(C) = p(W_0) = p(W) = 1/3$. Furthermore, as p (X = X_{obs}) is the same for all classes, Eq. (2) can be rewritten as:

$$P(\omega_i|X = X_{obs}) = Kp(X = X_{obs}|\omega_i) \tag{2}$$

where K is a constant for all classes, is in Eq. (3):

$$K = \frac{1}{3p(X=X_{obs})} \tag{3}$$

The likelihood function for each class is derived from the training data using a multivariate Gaussian model. For the observed feature vector $[\rho_{HV}, \rho_{12}, Z_{DR}]^T$, the joint likelihood is defined in Eq. (4):

$$P(X = X_{obs}|\omega_i) = p(\rho_{hv}, \rho_{12,}Z_{DR}|\omega_i). \tag{4}$$

where $p(X|\omega_i)$ represents the class-conditional probability density function (PDF) estimated from the joint feature space.

$p(X=X_{obs}|\omega i)$ is calculated for all classes, and the class corresponding to the maximum probability value will be selected as the classification decision. Thus, we can infer that the Bayesian classifier assigns X=X_{obs} to C only if, as mentioned in Eq. (5):

$$p(X = X_{obs}|C > p(X = X_{obs}|\omega_0) \text{ and } p(X = X_{obs}|C) > p(X = X_{obs}|W) \quad (5)$$

All posterior probabilities that a radar gate is clutter or weather are calculated using the probability density functions (PDFs) of these discriminants, derived from training data. The DPDS method is effective because it combines polarimetric and temporal information, thereby increasing detection probability and reducing false alarm rates, particularly for ambiguous discriminants.

Discriminant Functions. The Bayesian classifier makes its decision based on a set of discriminant functions derived from the radar data. These functions are chosen to maximise the statistical separation between the three classes. The discriminants used in the DPDS algorithm are:

1. Dual-Polarisation (DP) Discriminants describe the microphysical properties of the scatterers:
   (a) The co-polar cross-correlation coefficient (ρ_{hv}) measures the consistency between horizontally and vertically polarised returns. Weather echoes typically exhibit high ρ_{hv} values (>0.95), whereas clutter echoes exhibit lower, more variable values. It is defined as mentioned in Eq. (6) and Eq. (7):

$$\rho_{hv1} = \frac{\left|\frac{1}{M}\sum_{m=1}^{M} V_{h1}(m)V_{v1}^{*}(m)\right|}{\sqrt{\left|\left|\frac{1}{M}\sum_{m=1}^{M} V_{h1}V_{h1}^{*}(m)\right|\left|\frac{1}{M}\sum_{m=1}^{M} V_{v1}V_{v1}^{*}(m)\right|\right|}} \quad (6)$$

$$\rho_{hv2} = \frac{\left|\frac{1}{M}\sum_{m=1}^{M} V_{h2}(m)V_{v2}^{*}(m)\right|}{\sqrt{\left|\left|\frac{1}{M}\sum_{m=1}^{M} V_{h2}V_{h2}^{*}(m)\right|\left|\frac{1}{M}\sum_{m=1}^{M} V_{v2}V_{v2}^{*}(m)\right|\right|}} \quad (7)$$

   where V_{hm} and V_{vm} are the complex echo signal samples received from h(v) as the horizontally (vertically) polarised echo samples for the m-th pulse, *denotes the complex conjugate, and M represents the number of samples in a dwell time. Ground clutter remains relatively stable over time, resulting in ρ_{hv} values that are typically close to 1. Weather echoes, due to the random motion of precipitation particles, have lower values. There are two correlation coefficients, H and V polarisation, based on the two scans (ρ_{hv1} and ρ_{hv2}). Then, ρ_{hv} is used as the average of ρ_{hv1} and ρ_{hv2}, because the PDFs are nearly identical.

   (b) Differential Reflectivity (Z_{DR}), the ratio of horizontal to vertical reflectivity, is indicative of scatterer shape. Differential Reflectivity (Z_{DR}) measures the ratio of horizontally to vertically polarised power returns. It is beneficial for identifying the shape and type of hydrometeors (e.g., elongated raindrops versus nearly spherical hail) and is defined as Eq. (8):

$$Z_{DR} = 10log_{10}\left(\frac{\left|\frac{1}{M}\sum_{m=1}^{M} Vh_m V_h^{*}(m)\right|}{\left|\frac{1}{M}\sum_{m=1}^{M} V_V(m)V_V^{*}(m)\right|}\right) \quad (8)$$

   Ground clutter often has a Z_{DR} value near 0 dB or varies widely depending on the scatterer. Z_{DR} > 0 dB indicates that the dominant targets are wider horizontally than vertically, a common characteristic of larger raindrops that flatten into oblate spheroids as they fall. Z_{DR} ~ 0 dB suggests roughly spherical targets, typical for small raindrops, ice pellets, and tumbling hail. Z_{DR} < 0 dB is rare in natural precipitation but can occur with vertically elongated targets, indicating clutter or calibration issues.

   (c) Power Ratio (PR) is defined as the ratio, in decibels (dB), between the coherent power (the power of zero spectral lines) and the incoherent power (the sum of power from all other spectral lines) for each resolution volume. Because ground clutter is composed of deterministic scatterers that produce a coherent wave field, while randomly distributed hydrometeors (weather) yield an incoherent wave field, the PR can effectively discriminate between them. Ground clutter typically has a much higher PR value than weather signals. The Power Ratio is estimated from the time series I/Q data for both horizontal and vertical polarisations using the following Eq. (9) for PR_H and Eq. (10) for PR_V:

$$PR_H = 10log_{10}\left[\frac{\left|\frac{1}{M}\sum_{m=1}^{M} V_h(m)\right|^2}{\frac{1}{M}\sum_{m=1}^{M}|V_h(m)|^2 - \left|\frac{1}{M}\sum_{m=1}^{M} V_h(m)\right|^2}\right] \quad (9)$$

$$PR_V = 10log_{10}\left[\frac{\left|\frac{1}{M}\sum_{m=1}^{M} V_V(m)\right|^2}{\frac{1}{M}\sum_{m=1}^{M}|V_V(m)|^2 - \left|\frac{1}{M}\sum_{m=1}^{M} V_V(m)\right|^2}\right] \quad (10)$$

   Where the complex voltage samples Vh and Vv represent the resolution volumes in horizontal and vertical polarisations, respectively. M represents the number of pulses within the dwell time. PR_H and PR_V are used because they can be easily obtained from time-series samples, which are computationally efficient and physically meaningful. Ground clutter, characterised by almost zero Doppler velocity and a narrow spectrum width, is expected to exhibit larger PR_H and PR_V values than weather signals. Additionally, PR_H and PR_V of ground clutter in mechanical scans are lower than those in electronic scans because the time series samples within the dwell time of an electronic scan are more highly correlated.

   Although PR can be derived from Z_{DR} using Equations (9) and (10), it was excluded from the final Bayesian model due to its numerical instability. Under low Signal-to-Noise Ratio

(SNR) conditions prevalent in the Sidoarjo region, extreme Z_{DR} values resulted in PR spanning non-physical orders of magnitude, thereby diminishing the classifier's robustness compared to using Z_{DR} directly.

2. Dual-Scan (DS) Discriminant describes the temporal stability of the scatterers with Scan-to-Scan Correlation Coefficient (ρ_{12}) calculated from the complex (I/Q) time-series data of two consecutive scans at the same range gate. For a specific radar range gate, let $V_h(t_1)$ and $V_v(t_2)$ be the time series of complex radar signals from the horizontal and vertical channels during scan 1 and scan 2, respectively. Stationary targets (clutter) exhibit high correlation ($\rho_{12}\approx 1.0$), whereas moving hydrometeors (weather) show very low correlation ($\rho_{12}\approx 0$), as defined in Eq. (11):

$$\rho_{12,HV} = \frac{\left|\frac{1}{M}\sum_{m=1}^{M} V_{h1}(m) V_{v2}^{*}(m)\right|}{\sqrt{\left|\frac{1}{M}\sum_{m=1}^{M} V_{h1} V_{h1}^{*}(m)\right|\left|\frac{1}{M}\sum_{m=1}^{M} V_{v2} V_{v2}^{*}(m)\right|}} \quad (11)$$

The Surabaya weather radar meticulously collected the I/Q training and testing datasets at varying times and under distinct meteorological conditions. This meticulous approach was undertaken to ensure the classification's robustness and unbiasedness. The training dataset was exclusively utilised to estimate the PDFs of the Bayesian discriminant classifier. An independent dataset was reserved for testing and validation purposes.

The training dataset comprised four radar volume scans acquired on October 4, 2025. Two scans were collected under clear-air conditions at an elevation angle of 0.40° at 15:14:05 UTC (Scan 1) and 15:15:28 UTC (Scan 2) and were used to represent ground clutter. Two additional scans were acquired under cloudy but non-precipitating conditions at an elevation angle of 1.50° at 15:16:41 UTC (Scan 3) and 15:17:57 UTC (Scan 4) and were used to represent weather echoes. These four scans comprised the training dataset used to estimate the Bayesian classifier's statistical parameters.

The testing dataset was collected during an independent observation period that commenced on November 1, 2025. This period encompassed four scans conducted at identical elevation angles and scanning strategies as those employed in the training data. Two of these scans were performed at an elevation angle of 0.40° (16:01:29 UTC and 16:02:51 UTC), simulating clutter conditions. In comparison, the other two were conducted at an elevation angle of 1.50° (16:04:03 UTC and 16:05:19 UTC), simulating weather echoes. This temporal separation guarantees that the classifier's performance is assessed under novel atmospheric conditions, thereby mitigating the risk of information leakage between the training and testing phases.

The 83-second interval between consecutive azimuthal scans in the VCP 88888 strategy compromises temporal coherence, particularly for rapidly evolving tropical convection. In contrast, stationary ground clutter remains highly correlated ($\rho_{12} \approx 1.0$) over this period, meteorological echoes undergo significant decorrelation due to hydrometeor advection and internal storm turbulence. This interval yields a PDF of ρ_{12} for the Weather (W) class that is skewed toward lower values compared with those from shorter scan intervals used in experimental setups. Despite this decorrelation, the Bayesian classifier effectively utilises this 'decorrelation signature' as a discriminant to separate moving weather from stationary clutter.

To enhance data quality, I/Q samples underwent filtering before feature extraction. Weather data were filtered using a Signal-to-Noise Ratio (SNR) threshold of 20 dB, effectively eliminating low-SNR samples characterised by noise. For clutter data, resolution volumes with a mean Doppler velocity exceeding 1 ms^{-1} and a Clutter-to-Noise Ratio (CNR) below 3 dB were excluded to mitigate contamination from moving objects such as birds or vehicles.

From the cleaned I/Q data, polarimetric radar moments, including reflectivity (Z), differential reflectivity (Z_{DR}), co-polar correlation coefficient (ρ_{HV}), Doppler velocity, and power ratio (PR), were computed using coherent integration over a fixed cohesive processing interval (CPI). These features were subsequently utilised to estimate class-conditional Gaussian probability density functions for each class (W, W_0, and C).

The Bayesian classifier was trained exclusively on the training dataset, and classification was subsequently applied to the independent test dataset. This separation ensures a statistically valid assessment of the classifier's generalisation performance across diverse atmospheric conditions.

For a given range gate with a set of observed discriminant values X_O, the Bayesian classifier computes the conditional probability of those observations belonging to each class: $p(X_O|C)$, $p(X_O|W_0)$, and $p(X_O|W)$. These probability density functions (PDFs) are pre-determined from the extensive training dataset. The final classification is made according to the maximum likelihood rule: the echo is classified as clutter if $p(X_O|C)$ is greater than both $p(X_O|W_0)$ and $p(X_O|W)$.

Benchmark Algorithms for Comparison. To rigorously assess the performance of the DPDS algorithm, its results were compared against two established benchmark algorithms implemented using the same dataset:

1. DP-Only, a Bayesian classifier identical in structure to the DPDS algorithm but using only the Dual-Polarisation discriminants (ρ_{HV}, Z_{DR}, PR).
2. DS-Only, a simple classifier that identifies clutter based on a threshold applied solely to the scan-to-scan correlation coefficient (ρ_{12}).
3. DPDS, a Bayesian classifier using the Dual-Polarisation and dual scan discriminants (ρ_{HV}, ρ_{12}, Z_{DR}).

An optimal Bayesian classifier takes the vector of these three observed discriminant functions, (Z_{DR}, ρ_{HV}, ρ_{12}), as input, then uses them to decide if a radar gate contains clutter or weather based on the discriminant function. The three classes of echoes being considered are: (1) Clutter (C) for narrow band zero Doppler velocity; (2) Narrow-Band Zero Velocity Weather (W_0) where $|Vr| \leq 2$ m/s and sv≤ 2 m/s; and (3) Non-Zero Velocity Weather (W) where $|V| > 2$ m/s and W > 2 m/s. Vr and sv represent the mean Doppler velocity and the spectrum width of weather, respectively.

The DPDS algorithm is summarised in the following steps:

1. Calculate the Signal-Noise-to-Ratio (SNR) for the current gate. If SNR < 20 dB, the current gate is considered to lack a significant weather signal, and the SNR is *computed* for the next range gate. Otherwise, proceed to step 2.

2. Compute the three observed discriminant functions for the current gate. Calculate $p(X=X_{obs}|C)$, $p(X=X_{obs}|W0)$, and $p(X=X_{obs}|W)$ for the observed data.

3. If $p(X=X_{obs}|C) > p(X=X_{obs}|W0)$ and $p(X=X_{obs}|C) > p(X=X_{obs}|W)$ for the current gate, the data is considered clutter contaminated. Otherwise, the data is not contaminated, and the process is repeated for the next gate by returning to step 1.

Table 3. Confusion Matrix

	Predicted Clutter	***Predicted Weather***
Actual Clutter	True Positive (TP)	False Negative (FN)
Actual Weather	False Positive (FP)	True Negative (TN)

Evaluate the DPDS algorithm results. To assess the efficacy of a DPDS clutter-detection algorithm, a quantitative evaluation framework is essential. The goal is to evaluate the algorithm's ability to accurately identify and eliminate ground clutter while preserving genuine weather signals. An effective evaluation methodology uses a labelled dataset in which each radar gate is classified as either "clutter" or "weather". Quantitative evaluation relies on a confusion matrix to derive standard metrics that quantify detection performance, as shown in Table 3.

Using the values from this matrix, we can calculate the key performance metrics:

- The Probability of Detection (PoD), a measure of the proportion of actual clutter correctly identified by the algorithm, indicates improved clutter suppression. It is calculated as mentioned in Eq. (12):

$$PoD = \frac{TP}{TP+FN} \tag{12}$$

- The False Alarm Ratio (FAR), or False Discovery Rate (FDR), measures the proportion of predicted clutter that is actually meteorological contamination. The FAR is calculated as mentioned in Eq. (13):

$$FAR = \frac{FP}{TP+FP} \tag{13}$$

where FP represents weather echoes incorrectly predicted as clutter, and TP represents correctly identified clutter.

- Accuracy, a measure of the overall proportion of correctly classified radar gates (both clutter and weather), is calculated as Eq. (14):

$$Accuracy = \frac{TP+TN}{TP+TN+FP+FN} \tag{14}$$

3. Results and Discussion

Overview of Experimental Setup. This study evaluates the performance of a dual-polarisation–dual-scan (DPDS) clutter-discrimination framework using real weather radar observations from a C-band Doppler dual-polarisation radar in Surabaya, Indonesia. The primary objective is to quantify the contributions of polarimetric consistency and temporal coherence to the reliable identification of clutter under operational scanning conditions.

The dataset comprises raw in-phase and quadrature (I/Q) time-series measurements acquired during routine volumetric scanning. The radar operates at a wavelength of approximately 5.3 cm and performs azimuthal scans at multiple elevation angles. For this study, two low-elevation sweeps—0.4° and 1.5°—were selected to optimise sensitivity to ground clutter while ensuring adequate spatial coverage. Observations were conducted on October 4, 2025, and November 1, 2025, resulting in two consecutive scans per elevation angle and four datasets per observation day. This configuration enables both single-scan (DP) and dual-scan (DS) analyses.

Each radar volume comprises approximately 90,000 to 100,000 transmitted pulses, depending on the scan geometry and the antenna's rotation speed. The raw I/Q data are stored per pulse and per range gate, enabling the complete reconstruction of polarimetric radar moments. To mitigate near-field effects and beam-broadening artefacts, only gates located between 2km and 30km from the radar were considered. This range interval aligns with previous studies and represents a compromise between minimising near-range contamination and preserving adequate ground-clutter signatures.

To reduce noise and stabilise polarimetric estimates, radar moments were computed over coherent processing intervals (CPIs). A CPI is defined as the number of consecutive pulses averaged coherently. Multiple CPI lengths—16, 32, 64, and 128 pulses—were evaluated to assess the impact of temporal averaging on the stability of polarimetric parameters and clutter detectability. Each CPI corresponds to one effective radar "ray" in the processed dataset.

For each CPI, the following radar moments were derived: horizontal and vertical reflectivity (Zh, Zv), differential reflectivity (Z_{DR}), co-polar correlation coefficient (ρ_{HV}), differential phase (Φ_{DP}), radial velocity (Vr), and spectral width (σv). Using these quantities, three clutter identification strategies were implemented: (1) Dual-Polarisation (DP only) — based solely on polarimetric consistency within a single scan; (2) Dual-Scan (DS only) — based on temporal stability between two consecutive scans; and (3) Dual-Polarisation Dual-Scan (DPDS) — a combined criterion requiring both polarimetric coherence and temporal consistency. This experimental configuration enables a systematic investigation of how CPI length, elevation angle, and temporal coherence influence clutter detection performance in operational weather radar observations.

Spectral Characteristics of the Observed Data

To quantitatively evaluate the spectral behaviour of meteorological and non-meteorological echoes, the PDFs of Doppler velocity (v_r), spectral width (σ_v), and co-polar correlation coefficient (ρ_{HV}) were analysed using the processed radar moments. Fig.2 (a-d) presents the PDFs derived from the 0.4° and 1.5° elevation scans for both observation dates (October 4 and November 1, 2025), using CPI lengths of 16, 32, 64, and 128 pulses. In all cases, the velocity distributions are centred near 0 ms^{-1}, suggesting the predominance of stationary or quasi-stationary scatterers in the observed scenes. At shorter integration lengths (CPI = 16), the velocity distribution exhibits broader tails, with values extending up to approximately ±10–15 ms^{-1}. This behaviour reflects increased phase noise and reduced temporal coherence at short integration times. As CPI increases to 32 and 64 pulses, the velocity distribution narrows significantly, and extreme values become less frequent. For CPI = 128, the distribution becomes highly concentrated around zero, indicating strong temporal averaging and the suppression of random-phase fluctuations. Quantitatively, the standard deviation of Doppler velocity decreases from approximately 4–5 ms^{-1} at CPI = 16 to below 2 ms^{-1} at CPI = 128, demonstrating the stabilising effect of longer coherent integration. The spectral width distributions further highlight the impact of CPI length on spectral stability. For CPI = 16, spectral width values commonly exceed 3–4 ms^{-1}, indicating significant Doppler spectrum broadening due to noise, turbulence, and beam-filling effects. The behaviour of ρ_{HV} further supports these observations. At short CPI (16 pulses), ρ_{HV} exhibits a wide distribution, including a substantial number of low-correlation values (<0.7), indicative of decorrelation caused by noise and limited averaging. As CPI increases to 32 and 64 pulses, the ρ_{hv} distribution becomes increasingly concentrated at higher values (0.85–1.0), indicating improved phase coherence between horizontal and vertical polarisation channels. For CPI = 128, most samples exceed 0.95, suggesting highly stable scattering behaviour. As CPI increases from 16 to 128 pulses, the standard deviation of Doppler velocity decreases, and the ρ_{hv} distribution becomes more concentrated at higher values.

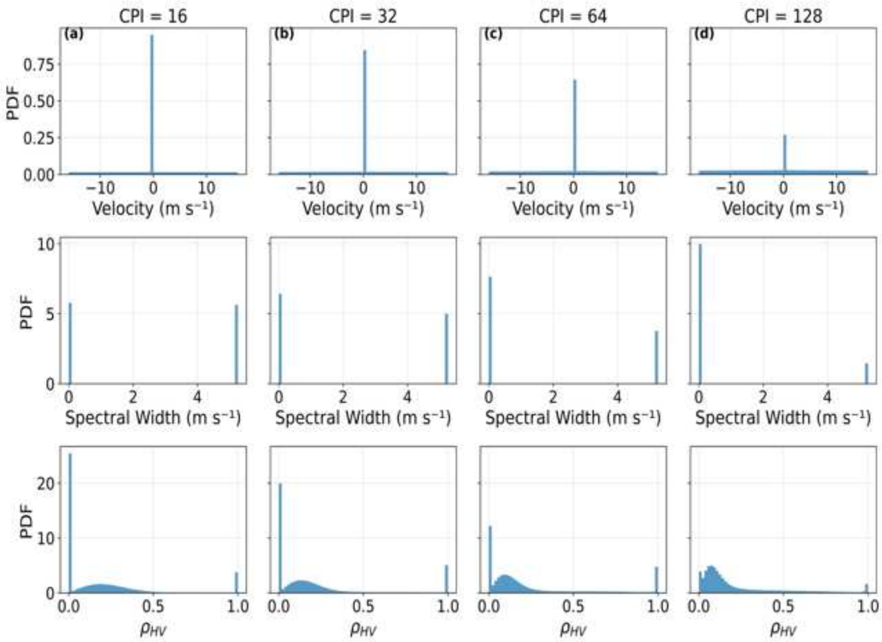

Figure 2. Effect of CPI on Doppler and Polarimetric Radar Moments.

Statistical Characteristics of Polarimetric Parameters for Clutter and Weather Echoes for DP-Only. Fig. 3 illustrates the PDF of the co-polar cross-correlation coefficient (ρ_{hv}) obtained through the DP-only classification approach. This method exclusively utilises polarimetric variables for echo classification, excluding dual-scan or Doppler-based information. The resulting PDFs exhibit a distinct separation between echo types. Clutter echoes (C) are characterised by a wide distribution of low ρ_{hv} values, which reflects the depolarising nature and heterogeneous scattering properties of non-meteorological targets. Zero-velocity weather echoes (W_0) exhibit intermediate to high ρ_{hv} values, indicating meteorological scattering with limited turbulence and weak radial motion, leading to reduced variability in polarimetric correlation.

In contrast, weather echoes (W) demonstrate a sharply peaked distribution near $\rho_{hv} \approx 1$, consistent with homogeneous hydrometeor populations and well-correlated horizontal and vertical backscattered signals. These distributions confirm that ρ_{hv} alone provides robust discriminatory capability between meteorological and non-meteorological echoes. However, the overlap between the W_0 and W classes underscores the inherent limitation of the DP-only approach for distinguishing weak-motion weather echoes from other meteorological returns when Doppler or dual-scan information is not employed.

Fig. 4 presents the PDF of differential reflectivity (Z_{DR}). The Z_{DR} distribution for weather echoes (W) exhibits a sharp, symmetric peak centred near 0 dB, indicating predominantly spherical or weakly oblate hydrometeors and a homogeneous scattering population. This behaviour aligns with stratiform or widespread precipitation, characterised by relatively uniform particle shapes and orientations. This behaviour aligns with stratiform or widespread precipitation, characterised by relatively uniform particle shapes and orientations. Zero-velocity weather echoes (W_0) exhibit a broader Z_{DR} distribution, extending towards both negative and positive values.

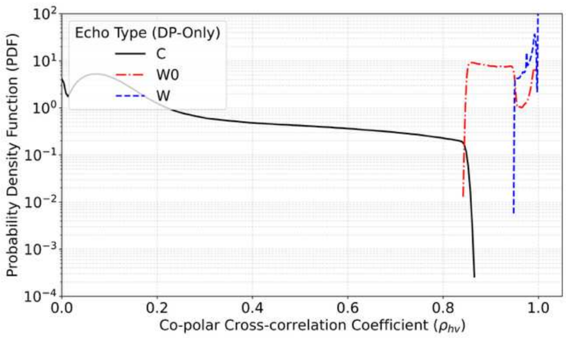

Figure 3. PDFs of the ρ_{hv} for clutter (C), weather (W), and zero-velocity weather (W_0) using DP-Only.

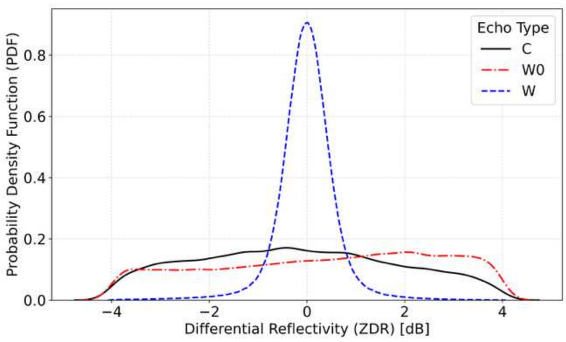

Figure 4. PDFs of the Z_{DR} for clutter (C), weather (W), and zero-velocity weather (W_0) using DP-Only.

This reflects a mixture of weakly turbulent meteorological echoes with limited radial motion, where variations in hydrometeor shape, size, and orientation become more pronounced despite the absence of significant Doppler velocity. This behaviour aligns with stratiform or widespread precipitation, characterised by relatively uniform particle shapes and orientations. Zero-velocity weather echoes (W_0) exhibit a broader Z_{DR} distribution, extending towards both negative and positive values. This reflects a mixture of weakly turbulent meteorological echoes with limited radial motion, where variations in hydrometeor shape, size, and orientation become more pronounced despite the absence of significant Doppler velocity. In contrast, clutter echoes (C) exhibit the widest Z_{DR} distribution, spanning a broad range of negative and positive values. This broad spread is indicative of non-meteorological targets with highly irregular shapes and orientations, such as ground clutter or artificial objects, which generate inconsistent polarimetric backscatter responses.

Fig. 5 illustrates the PDF of the Power Ratio (PR), which serves as an independent spectral discriminant to Z_{DR}. ZDR characterises scatterer shape based on polarisation power returns, whereas PR distinguishes the coherent nature of ground clutter from the incoherent signals of randomly moving hydrometeors. However, as shown in Fig. 5, the PR distribution for the DP-only method exhibits numerical instability at low SNR, leading to extreme Z_{DR} values that were previously erroneously associated with its calculation. Consequently, the framework was refined to treat these as distinct physical variables. It demonstrates that PR is highly sensitive to extreme Z_{DR} values. In low-SNR and clutter-contaminated regions, Z_{DR} can attain unrealistically large magnitudes, resulting in non-physical PR values spanning several orders of magnitude. Consequently, the PDF of PR becomes numerically unstable and fails to accurately reflect the meaningful scattering characteristics. Although the PR can be derived from differential reflectivity, its PDF is highly sensitive to extreme Z_{DR} values, particularly under low SNR conditions. Consequently, PR-based PDFs may exhibit numerical instability and are less robust than Z_{DR}-based representations. Therefore, Z_{DR} is adopted as the primary polarimetric descriptor in the DP-only analysis.

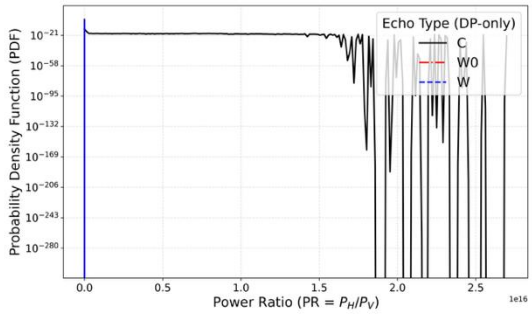

Figure 5. PDFs of the PR for clutter (C), weather (W), and zero-velocity weather (W_0) using DP-Only.

Fig. 6 presents the normalised confusion matrix for the dual-polarisation (DP-only) classification method. In this approach, echo classification relies exclusively on polarimetric variables, primarily the ρ_{hv} and Z_{DR}, without incorporating Doppler spectral or temporal information. The DP-only method demonstrates moderate capability for identifying clutter echoes (C), correctly classifying approximately 71% of actual clutter. However, a substantial fraction of clutter is misclassified as weather (19%) or zero-velocity weather (9%), indicating that polarimetric signatures alone are insufficient to fully discriminate non-meteorological targets with complex scattering characteristics. For zero-velocity weather echoes (W_0), the classification performance is notably weak. Only about 4% of W_0 echoes are correctly identified, while the majority (85%) are misclassified as clutter. This result highlights the fundamental limitation of the DP-only approach in distinguishing weak-motion meteorological echoes from clutter, as both echo types often exhibit similarly high ρ_{hv} values and overlapping Z_{DR} distributions. The most pronounced limitation is observed for weather echoes (W), where nearly 99% actual weather samples are incorrectly classified as clutter. This severe misclassification indicates that, in the absence of Doppler or temporal discriminants, DP-only features do not provide sufficient information to separate dynamically evolving meteorological echoes from stationary or quasi-stationary targets.

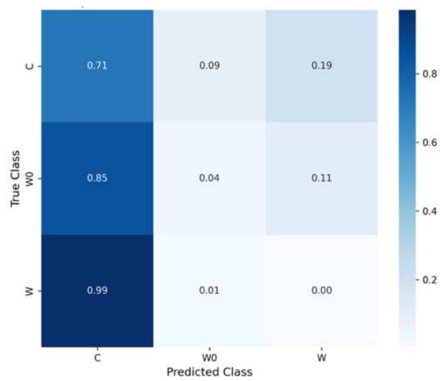

Figure 6. Confusion matrix using DP-Only

Statistical Characteristics of Polarimetric Parameters for Clutter and Weather Echoes for DS-Only. Fig. 7 presents the PDFs of the dual-scan cross-correlation coefficient (ρ_{12}) derived using the DS-only framework. Weather echoes (W) exhibit high temporal coherence, with PDFs concentrated towards large ρ_{12} values, reflecting consistent scatterer (C) evolution between consecutive scans. Zero-velocity weather (W_0) shows a similar but slightly broader distribution, indicating reduced advection. Ground clutter produces a pronounced peak near unity, consistent with the presence of stationary targets. The substantial overlap between clutter and zero-velocity weather highlights the inherent limitation of DS-only approaches, which lack microphysical information to distinguish stationary meteorological echoes from non-meteorological targets.

Fig.8 shows the confusion matrix derived from the DS-only classification. The result reveals that dual-scan temporal (ρ_{12}) coherence provides reasonable discrimination of meteorological echoes but demonstrates limited capability to suppress ground clutter. Weather (W) and zero-velocity weather (W_0) echoes are accurately identified with relatively high detection probabilities (approximately 79% and 74%, respectively), indicating that their temporal correlation characteristics are sufficiently distinct from rapidly decorrelating noise. Conversely, only approximately 7% of clutter (C) echoes are correctly classified, with the majority being misidentified as weather. This misclassification arises because stationary or slowly varying ground targets often exhibit strong inter-scan correlation, which closely resembles the temporal behaviour of precipitation echoes. These findings indicate that a DS-only framework is inadequate for reliable clutter rejection and emphasise the importance of incorporating dual-polarisation information to improve echo classification performance.

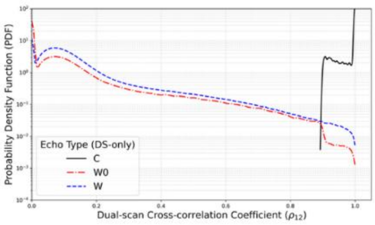

\

Figure 7. PDFs of the ρ_{12} for clutter (C), weather (W), and zero-velocity weather (W_0) using DP-Only.

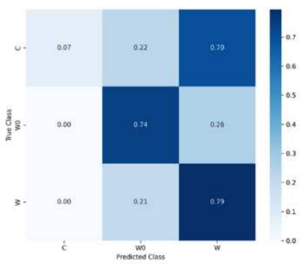

Figure 8. Confusion matrix using DS-Only

Statistical Characteristics of Polarimetric Parameters for Clutter and Weather Echoes for DPDS. Following physical pre-classification, a Bayesian maximum a posteriori (MAP) decision rule was employed using a multivariate Gaussian model of the joint feature space (ρ_{HV}, ρ_{12}, Z_{DR}). Class-conditional likelihoods and prior probabilities were estimated from the training dataset, resulting in a Bayes-optimal classifier under the assumption of equal misclassification costs.

The PDFs of the co-polar cross-correlation coefficient (ρ_{hv}) derived from the DPDS classification framework demonstrate distinct statistical separation among clutter (C), zero-velocity weather (W_0), and weather echoes (W) as shown in Fig.9. Clutter echoes exhibit a broad distribution with significantly lower ρ_{hv} values, reflecting the heterogeneous scattering characteristics of non-meteorological targets. In contrast, weather echoes (W) exhibit a sharply peaked distribution concentrated near unity ($\rho_{hv} \approx 1$), consistent with highly homogeneous hydrometeor populations and stable.

Dual-Polarisation returns. The W_0 class occupies an intermediate regime, characterised by elevated ρ_{hv} values comparable to those of meteorological echoes, but with increased spread, indicating weak turbulence and near-zero radial velocity conditions that partially resemble clutter. The partial overlap between W_0 and C at lower ρ_{hv} values underscores the inherent ambiguity of zero-velocity weather echoes.

Fig.10 shows the PDFs of the dual-scan cross-correlation coefficient (ρ_{12}) derived from the DPDS classification framework. Clutter echoes exhibit a broad distribution with relatively high ρ_{12} values, reflecting strong temporal persistence between consecutive scans due to stationary or quasi-stationary non-meteorological targets. This characteristic leads to elevated dual-scan correlation despite low meteorological relevance. Weather echoes (W) exhibit markedly different behavior, with the PDF skewed toward lower ρ_{12} values. This reduction in cross-scan correlation is consistent with rapidly evolving hydrometeor fields and advection-induced decorrelation between successive scans. The W_0 class occupies an intermediate regime, showing moderate ρ_{12} values that overlap with both clutter and weather distributions. This behavior is physically consistent with weakly advecting meteorological echoes characterized by near-zero radial velocity and limited temporal variability.

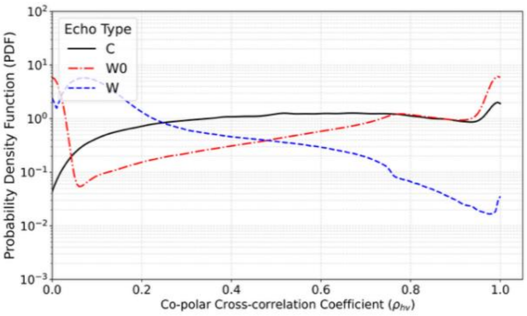

Figure 9. PDFs of the ρ_{hv} for clutter (C), weather (W), and zero-velocity weather (W_0) using DPDS.

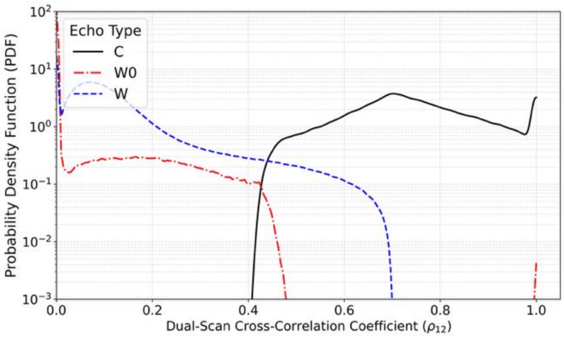

Figure 10. PDFs of the ρ_{12} for clutter (C), weather (W), and zero-velocity weather (W_0) using DPDS.

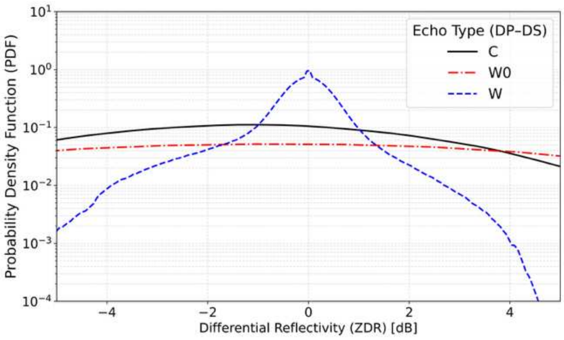

Figure 11. PDFs of the Z_{DR} for clutter (C), weather (W), and zero-velocity weather (W_0) using DPDS.

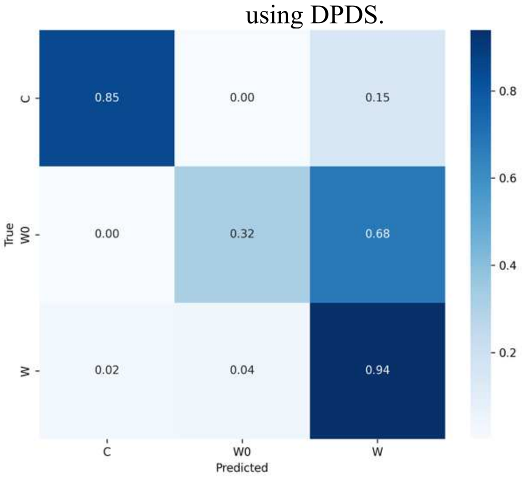

Figure 12. Confusion matrix using DPDS

The PDFs of Z_{DR} derived from the DPDS classification framework are shown in Fig.11. Weather echoes (W) exhibit a pronounced peak centred near $Z_{DR} \approx 0$ dB, indicating a predominance of near-spherical hydrometeors and well-mixed precipitation particles. The relatively narrow distribution reflects the physical homogeneity of meteorological scatterers and the effectiveness of the DPDS framework in isolating dynamically evolving weather echoes. The W_0 class displays a broader Z_{DR} distribution with moderate asymmetry, spanning both slightly negative and positive values. This behavior is consistent with weakly advecting meteorological echoes, in which partial beam filling, mixed-phase hydrometeors, or low signal-to-noise conditions introduce increased variability in differential reflectivity. Clutter echoes (C) exhibit the widest Z_{DR} spread, extending toward larger absolute values. This broad distribution reflects non-meteorological scattering mechanisms, including anisotropic targets and surface reflections, which produce highly variable polarisation signatures.

Fig. 12 shows the normalised confusion matrix for the proposed DPDS classification framework, demonstrating improved echo-type discrimination compared with single-source methods. Clutter (C) echoes are correctly identified with a probability of 0.85, indicating strong classification performance. Notably, only a minimal fraction (0.15) of clutter is misclassified as weather, suggesting limited residual contamination. In the zero-velocity weather (W_0) class, 32% of samples are correctly classified, while the remaining 68% are predominantly assigned to the weather (W) class. This behavior reflects the inherent physical similarity between W_0 and low-velocity weather echoes, particularly in polarimetric signatures, despite the inclusion of temporal coherence information.
Nevertheless, the absence of misclassification of W_0 as clutter highlights the robustness of the DPDS framework in preserving the integrity of meteorological echoes. Weather (W) echoes exhibit the highest classification performance, with a correct detection rate of 0.94. Misclassification into clutter (0.02) and W_0 (0.04) remains minimal, confirming that the joint exploitation of polarimetric consistency (ρ_{hv}, Z_{DR}) and inter-scan coherence (ρ_{12}) effectively isolates dynamically evolving meteorological echoes. Overall, the DPDS confusion matrix indicates that integrating dual-polarisation and dual-scan information improves class separability and produces a more physically consistent echo classification than DP-only or DS-only frameworks.

Quantitative evaluation by using the DP-Only, DS-Only, and DPDS algorithms. Table 4 presents a comparative analysis of the performance of the DP-only, DS-only, and DPDS classification methods in terms of POD, FAR, and accuracy for clutter (C), zero-velocity weather (W_0), and weather (W) echoes, derived using a Coherent Processing Interval (CPI) of 64 pulses.

The DP-only approach demonstrates limited discrimination capability, particularly for weather echoes, as evidenced by low POD values for W (0.003) and high FAR for clutter and weather classes, indicating significant ambiguity when relying solely on dual-polarimetric variables. Conversely, the DS-only method significantly improves meteorological echo detection, achieving high POD values for W_0 (0.743) and W (0.795) while substantially reducing FAR. This result demonstrates the efficacy of temporal coherence and Doppler information in distinguishing weather from non-weather targets. The proposed DPDS approach delivers the most balanced and robust performance across all classes, achieving the highest PODs for clutter (0.850) and weather (0.939), while maintaining high classification accuracy (>0.77 across all classes). These findings indicate that dual-polarisation and dual-scan information act as complementary sources of discrimination, improving echo classification reliability compared with DP-only or DS-only schemes. The DPDS framework achieves a high overall Accuracy of 0.982, despite a FAR of 0.749 for the clutter class.

Table 4. All performance metrics (POD, FAR, and Accuracy) by using the DP-only, DS-only, and DPDS algorithms were derived using a CPI of 64 pulses

Method	Class	POD	FAR	Accuracy
DP-only	C	0.714	0.995	0.054
	W_0	0.039	0.460	0.741
	W	0.003	0.934	0.239
DS-only	C	0.072	0.002	0.979
	W_0	0.743	0.686	0.789
	W	0.795	0.060	0.778
DPDS	C	0.850	0.749	0.982
	W_0	0.320	0.256	0.794
	W	0.939	0.205	0.778

This apparent discrepancy is due to the dataset's class distribution. Because moving weather (W) echoes are significantly more frequent than clutter (C) echoes in the Surabaya C-band observations, the high POD for weather (0.939) dominates the accuracy calculation. The 0.749 FAR indicates that while the algorithm is 'aggressive' in identifying clutter (often capturing stable tropical rain due to the 83-second scan interval), the total number of correct weather identifications (True Negatives) is large enough to ensure the overall reliability of the classification field.

PDFs Comparison: DP-only vs DPDS (ρ_{hv}), DS-only vs DPDS (ρ_{12}), and DP-only vs DPDS (Z_{DR}). The PDFs of ρ_{HV} exhibit distinct differences between the DP-only and DPDS classification frameworks. In the DP-only approach, the weather (W) class exhibits a pronounced concentration near $\rho_{HV} \approx 1$, whereas clutter (C) and zero-velocity weather (W_0) display broader, partially overlapping distributions, indicating limited separability when relying solely on polarimetric information. Conversely, the DPDS framework produces sharper and more distinct ρ_{HV} PDFs across all echo types. The incorporation of dual-scan information (ρ_{HV}) effectively suppresses misclassified weather echoes within the clutter and W_0 classes, thereby reducing overlap and enhancing class discrimination. This demonstrates that while ρ_{HV} alone captures hydrometeor uniformity, its discriminatory power is significantly enhanced when combined with the temporal consistency provided by the DPDS method.

The PDF representations of the dual-scan cross-correlation coefficient (ρ_{12}) elucidate fundamental distinctions between the DS-only and DPDS classification methodologies. Within the DS-only framework, the ρ_{12} distributions of clutter (C) and weather (W) exhibit considerable overlap, particularly at moderate-to-high correlation values, leading to ambiguity in echo separation. Zero-velocity weather (W_0) also encompasses a wide range of ρ_{12} values, reflecting the restricted capacity of DS-only features to characterise echo physical properties fully. Conversely, the DPDS approach generates more compact and physically consistent ρ_{12} PDFs. Weather echoes intensely concentrated at high ρ_{12} values, while clutter and W_0 are more distinctly segregated toward lower correlations. This enhancement highlights the benefit of incorporating Dual-Polarisation variables, which constrain the DS-based classification and improve the physical interpretability of ρ_{12}.

The Z_{DR} PDFs further demonstrate the advantages of the DPDS framework over the DP-only method. In the DP-only classification, Z_{DR} distributions for clutter (C) and zero-velocity weather (W_0) exhibit wide spreads and significant overlap, particularly near-zero Z_{DR} values, which hinders their separability. Weather echoes (W) tend to cluster closer to 0 dB but still exhibit extended tails, indicating residual contamination from non-meteorological echoes. When dual-scan information is incorporated into the DPDS framework, the Z_{DR} PDFs become notably more compact and class-dependent. The weather class exhibits a sharper peak around $Z_{DR} \approx 0$ dB, while clutter and W_0 distributions are better confined to their respective ranges. This enhanced separation indicates that the DPDS method not only stabilises Z_{DR} statistics but also reduces ambiguities inherent in DP-only classification by exploiting temporal coherence across consecutive scans.

Excluding the Power Ratio (PR) was necessary to maintain classifier stability. While C-band attenuation can affect signal intensity, the primary driver for PR instability in this study was low Signal-to-Noise Ratio (SNR) conditions. In regions with low SNR, differential reflectivity (Z_{DR}) estimates often attain unrealistically large or small magnitudes, leading to non-physical PR values spanning several orders of magnitude. Because PR-based probability density functions (PDFs) proved less robust than ZDR-based representations under these conditions, the framework was optimised to rely on Z_{DR} and ρ_{HV} for microphysical discrimination.

The DPDS framework achieves a W_0 POD of 0.320, which is lower than the DS-only approach (0.743). This is attributed to the Bayesian classifier's stringent requirement for both high temporal correlation (ρ_{12}) and high polarimetric coherence (ρ_{HV}). For W_0 signals, these dual constraints are more restrictive than a temporal-only threshold. Furthermore, the clutter FAR of 0.749 is primarily due to the 83-second scan interval. In Surabaya's tropical climate, stratiform rain patterns often exhibit high scan-to-scan correlation over this duration, causing the algorithm to misidentify them as stationary clutter.

The quantitative assessment reveals a clutter FAR of 0.749 for the DPDS framework. This relatively high value is fundamentally linked to the 83-second scan interval utilised in the operational VCP 88888 strategy. In the Sidoarjo/Surabaya region, tropical stratiform rain patterns frequently exhibit high temporal stability, maintaining high scan-to-scan correlation (ρ_{12}) even over periods exceeding one minute. Because the Bayesian classifier utilises ρ_{12} as a primary indicator of stationarity, these slowly evolving meteorological echoes can statistically overlap with the clutter class (C), leading to erroneous flagging of weather as clutter. Although this sensitivity increases the probability of detection (POD) for ground targets, further research is needed to investigate shorter scan intervals (< 60 s) to better decorrelate weather signals from the stationary infrastructure.

Confusion Matrices Comparison: DP-only, DS-only, and DPDS Classification. A comparative analysis of the confusion matrices reveals a progressive enhancement in echo classification performance from the DP-only approach to the DS-only approach, and ultimately, to the combined DPDS framework. The DP-only approach demonstrates limited discrimination capability, particularly for weather echoes (W), which are predominantly misclassified as clutter (C). This suggests that polarimetric information alone is insufficient to capture the temporal dynamics of meteorological echoes. While the DP-only approach achieves moderate clutter detection, its poor weather identification results in a high false-alarm rate and low overall reliability for operational classification.

In contrast, the DS-only method significantly improves the detection of weather echoes, achieving high correct classification rates for W and W_0 classes by utilizing inter-scan coherence and Doppler velocity information. However, the DS-only approach's performance deteriorates in clutter discrimination, with a substantial fraction of clutter echoes misclassified as weather, indicating that temporal coherence alone is insufficient to fully characterise non-meteorological targets. The proposed DPDS framework demonstrates the best overall performance across all classes, combining the strengths of both approaches. Clutter echoes are correctly identified with high probability, weather echoes achieve the highest detection rate, and misclassification between meteorological and non-meteorological classes is significantly reduced. Although some ambiguity persists between W_0 and W due to their inherent physical similarity, the DPDS confusion matrix confirms that integrating Dual-Polarisation and dual-scan information yields a more balanced, physically consistent, and robust echo classification than either the DP-only or DS-only methods.

Matrix Accuracy Comparison: DP-only, DS-only, and DPDS Classification. A comparative evaluation of the probability of detection (POD), false alarm rate (FAR), and classification accuracy reveals distinct performance disparities among the DP-only, DS-only, and combined DPDS approaches. The DP-only method exhibits limited detection capabilities for meteorological echoes, particularly for weather (W) and zero-velocity weather (W_0), as evidenced by exceptionally low POD values and high FAR. This behaviour reflects the inherent ambiguity of polarimetric signatures when Doppler and temporal coherence information are unavailable, leading to frequent misclassification of weather echoes as clutter.

The DS-only approach demonstrates a significant enhancement in detecting meteorological echoes, achieving high POD values for both W_0 and W with substantially reduced FAR. This improvement corroborates the strong discriminatory power of dual-scan coherence and Doppler-based features in distinguishing stationary clutter from moving weather targets. However, the DS-only scheme exhibits limited capability to accurately identify clutter, as reflected by the low POD for the clutter class, indicating residual overlap among W, W_0, and C signatures under low-motion conditions.

The proposed DPDS method consistently delivers the most balanced performance across all echo types. By jointly exploiting polarimetric diversity and inter-scan coherence, the DP–DS approach significantly enhances POD for clutter and weather while maintaining moderate FAR and high overall accuracy. These results demonstrate that integrating

Dual-Polarisation and dual-scan information provide complementary and synergistic benefits, yielding a more robust and reliable echo classification framework than either the DP-only or DS-only methods.

Operational Implications for the Surabaya Region. The DPDS framework's capability to achieve a POD of 0.939 for W echoes presents a significant advantage for QPE in the Surabaya region. Conventional clutter mitigation techniques frequently exhibit a low-velocity bias, inadvertently filtering out substantial, slow-moving tropical precipitation. By accurately preserving nearly 94% of meteorological signals, the DPDS framework mitigates the underestimation of rainfall rates. In flood-prone urban environments such as Surabaya, this high sensitivity improves hydrological model inputs and supports more reliable flash-flood forecasting during the monsoon season.

Effective ground clutter mitigation is particularly crucial at the Sidoarjo radar site, given Surabaya's densely populated urban environment. Tall buildings and industrial structures generate substantial 'urban noise,' which can obscure the initial stages of coastal convective cells developing over the Madura Strait. By achieving a clutter POD of 0.850, the DPDS framework effectively eliminates these non-meteorological returns. This 'cleaned' radar field enables meteorologists to identify the signatures of severe weather, such as gust fronts or rapid intensification, at an earlier stage. Consequently, the lead time for early warning systems is enhanced, providing residents in the coastal-urban interface with crucial additional minutes to prepare for high-impact weather events.

The exceptionally low POD for the DP-only method (0.003) serves as a critical finding that highlights the limitations of polarimetric-only classification in high-clutter urban environments. In the Surabaya C-band dataset, the PDFs for Z_{DR} and ρ_{HV} for W and C exhibit substantial overlap. Without the temporal anchor provided by the dual-scan correlation ρ_{HV}, the Bayesian classifier, when compelled to select solely based on polarimetric consistency, defaults to the more statistically dominant class (clutter) for echoes with low radial velocity. This 'polarimetric blindness' is precisely why integrating the DS framework is imperative, as it provides the secondary dimension needed to achieve the 0.939 POD observed in the final DPDS method.

4. Conclusion

The DPDS framework offers an effective approach to clutter mitigation in complex tropical environments such as Surabaya, albeit at the cost of a deliberate performance trade-off. In the context of clutter (C) detection, the DPDS method achieves a POD of 0.850, which represents an improvement of 13.6% over DP-only (0.714) and more than an order of magnitude over DS-only (0.072). Although the DPDS FAR for clutter (0.749) remains higher than that of DS-only (0.002), it yields a substantially higher classification accuracy of 0.982, surpassing both DP-only (0.054) and DS-only (0.979). This finding indicates that combining polarimetric and temporal decorrelation information significantly enhances clutter separability while maintaining overall classification reliability.

For zero-velocity weather (W_0) echoes, which represent the most challenging class due to their clutter-like characteristics, DPDS provides a balanced improvement. The DPDS approach achieves a POD of 0.320, which is substantially higher than the DP-only approach (0.039) but lower than the DS-only approach (0.743). However, DP–DS FAR to 0.256, corresponding to a 63% reduction compared to DS-only (0.686), while maintaining a comparable accuracy of 0.794. This result highlights that incorporating Dual-Polarisation constraints mitigates the over-classification of W_0 echoes observed in DS-only processing. Although the DPDS approach provides balanced improvements, the POD for W_0 (0.320) is lower than that of the DS-only method (0.743). This lower sensitivity indicates that the DPDS framework prioritises polarimetric consistency over detection of low-velocity weather, thereby reducing the misclassification of weather as clutter.

For moving weather (W) echoes—the primary drivers of convective rainfall—the framework demonstrates its most significant gains, achieving a Probability of Detection (POD) of 0.939. This represents a 313 -fold improvement over DP-only methods and a substantial increase over the 0.795 POD of DS-only approaches. While the detection rate for zero-velocity weather (W0) decreased to 0.320 (compared to 0.743 in DS-only), this reduction is a necessary consequence of the framework's stringent 'purity-first' logic. By requiring echoes to satisfy both temporal and polarimetric consistency, the DPDS method successfully filtered out the urban clutter that the DS-only method erroneously flagged as weather. This resulted in a 63% improvement in classification purity (reducing W0 FAR from 0.686 to 0.256). Ultimately, the DPDS framework preserves 93.9% of the most active meteorological signals while reducing urban noise in the identified weather field over the Surabaya metropolitan area, achieving an overall accuracy of 0.982.

Suggestion

Although the DPDS framework improves clutter discrimination, several aspects warrant further investigation. Future research should investigate the DPDS classifier's sensitivity to different scanning strategies and elevation angles. In particular, shorter scan intervals (e.g., 30–60 s) should be evaluated to refine the temporal coordination logic and improve the separability of quasi-stationary meteorological echoes across consecutive scans. The integration of additional discriminants, such as spectral width or differential phase (Φ_{DP}), may further enhance class separability under intricate meteorological conditions. Furthermore, extending the framework to incorporate adaptive or learning-based Bayesian priors or machine learning could improve performance under seasonally variable clutter characteristics. Finally, real-time implementation and extensive operational testing across multiple radar sites are recommended to evaluate computational efficiency and long-term resilience in diverse environments.

Acknowledgement

The authors would like to express their sincere appreciation to the Indonesian Meteorological, Climatological, and Geophysical Agency (BMKG), particularly the Juanda Meteorological Station, Surabaya, for providing access to the operational weather radar I/Q datasets used in this study. The authors acknowledge the support of the weather forecasting and technical teams during data acquisition and system configuration. The authors also thank Mr. Rendy and Mr. Jeff Olofson of Baron Weather Radar Company for their technical assistance.

This research was conducted as part of academic activities at IPB University, and the authors gratefully acknowledge the institutional support provided by the Department of Geophysics and Meteorology. Financial support for this research was provided by the Pusat Pengembangan Sumber Daya Manusia (PPSDM) of the BMKG, which is sincerely acknowledged.

References

[1] Y. Tian *et al.*, "An Operational and Real-Time Severe Weather Nowcasting System Based on Lightning Jumps: Introduction and Evaluation," *Advances in Meteorology*, vol. 2025, no. 1, p. 4280862, Jan. 2025, doi: 10.1155/adme/4280862.

[2] S. Torres, "Signal Processing Innovations at the National Severe Storms Laboratory: Improving the Quality and Timeliness of Data from Operational and Next-Generation Weather Radars," in *IGARSS 2024 - 2024 IEEE International Geoscience and Remote Sensing Symposium*, Jul. 2024, pp. 503–506. doi: 10.1109/IGARSS53475.2024.10640502.

[3] H. Zhou, X. Dong, X. Zhao, K. Cui, L. Zhu, and J. Lu, "Improved CLEAN-AP for Dual-Polarization Alternating Transmission Weather Radar," presented at the IEEE International Conference on Signal, Information and Data Processing, ICSIDP 2024, 2024. doi: 10.1109/ICSIDP62679.2024.10868685.

[4] J. E. E. Seltmann, "Weather Radar," in *Springer Handbooks*, 2021, pp. 841–900. doi: 10.1007/978-3-030-52171-4_30.

[5] M. Montopoli *et al.*, "Overview on Weather Radar Applications," presented at the 17th European Conference on Antennas and Propagation, EuCAP 2023, 2023. doi: 10.23919/EuCAP57121.2023.10133034.

[6] N. Nanding and M. A. Rico-Ramirez, "Precipitation Measurement with Weather Radars," in *Handb. Environ. Chem.*, vol. 102, Springer Science and Business Media Deutschland GmbH, 2021, pp. 235–258. doi: 10.1007/698_2019_404.

[7] Z. Chen, X. Liu, Z. Wu, and X. Wang, "The analysis of sea clutter statistics characteristics based on the observed sea clutter of Ku-band Radar," presented at the ISAP 2013 - Proceedings of the 2013 International Symposium on Antennas and Propagation, 2013, pp. 1183–1186. [Online]. Available: https://www.scopus.com/inward/record.uri?eid=2-s2.0-84894230654&partnerID=40&md5=1554c842bd74f8d5d19088af308e6352

[8] F. Maniraguha, A. Vodacek, E. Ndashimye, and G. Rushingabigwi, "Ground Clutter Mitigation and Insect Signature Detection for Polarimetric C-Band Doppler Weather Radar," presented at the 2021 11th IEEE Global Humanitarian Technology Conference, GHTC 2021, 2021, pp. 289–296. doi: 10.1109/GHTC53159.2021.9612449.

[9] H. P. Phyu, K. S. Lwin, T. T. Oo, and P. T. Aung, "Analysis on Ground Clutter Mitigation Using IIR Filter and Frequency Domain Filters for C-Band Phased Array Weather Radar," presented at the Proceedings of the 4th International Conference on Advanced Information Technologies, ICAIT 2020, 2020, pp. 48–52. doi: 10.1109/ICAIT51105.2020.9261791.

[10] X. Yao, M. Shen, D. Wu, and D. Zhu, "Wind turbine clutter suppression for weather radars by improved range-doppler domain joint interpolation in low SNR environments," *Progress In Electromagnetics Research M*, vol. 85, pp. 145–154, 2019, doi: 10.2528/pierm19070701.

[11] R. Bölz *et al.*, "Enhancing weather radar data by removing non-meteorological echoes, using neural networks trained on synthetic weather data," *EGUsphere*, vol. 2026, pp. 1–28, Mar. 2026, doi: 10.5194/egusphere-2026-992.

[12] "(PDF) Weather Radar Ground Clutter. Part I: Identification, Modeling, and Simulation," *ResearchGate*, Aug. 2025, doi: 10.1175/2008JTECHA1159.1.

[13] Y.-S. Kim, D. Schvartzman, R. D. Palmer, T.-Y. Yu, F. Nai, and C. Curtis, "A Clutter Mitigation Technique for Phased Array Weather Radar," presented at the IEEE International Symposium on Phased Array Systems and Technology, 2024. doi: 10.1109/ARRAY58370.2024.10880355.

[14] Z. Yan, C. Hu, K. Cui, R. Wang, Z. Yang, and C. Zhang, "Utilizing Range-Doppler Characteristics for Classifying Insect and Bird Echoes in Weather Radar," *IEEE Transactions on Geoscience and Remote Sensing*, vol. 63, pp. 1–13, 2025, doi: 10.1109/TGRS.2025.3583075.

[15] J. C. Hubbert, M. Dixon, S. M. Ellis, and G. Meymaris, "Weather Radar Ground Clutter. Part I: Identification, Modeling, and Simulation," *Journal of Atmospheric and Oceanic Technology*, vol. 26, no. 7, pp. 1165–1180, Jul. 2009, doi: 10.1175/2009JTECHA1159.1.

[16] Y. Cheng, J. Su, C. Xiu, and J. Liu, "Adaptive Clutter Intelligent Suppression Method Based on Deep Reinforcement Learning," *Applied Sciences*, vol. 14, no. 17, p. 7843, Sep. 2024, doi: 10.3390/app14177843.

[17] Y. Li, G. Zhang, R. J. Doviak, L. Lei, and Q. Cao, "A new approach to detect ground clutter mixed with weather signals," *IEEE Transactions on Geoscience and Remote Sensing*, vol. 51, no. 4, pp. 2373–2387, 2013, doi: 10.1109/TGRS.2012.2209658.

[18] F. Kong, Y. Zhang, and R. Palmer, "Wind Turbine Clutter mitigation for weather radar by Adaptive Spectrum Processing," in *2012 IEEE Radar Conference*, May 2012, pp. 0471–0474. doi: 10.1109/RADAR.2012.6212187.

[19] S. L. Durden and S. Tanelli, "Application of clutter suppression methods to a geostationary weather radar concept," *Progress In Electromagnetics Research Letters*, vol. 8, pp. 115–124, 2009, doi: 10.2528/PIERL09040910.

[20] D. A. Warde and S. M. Torres, "The Autocorrelation Spectral Density for Doppler-Weather-Radar Signal Analysis," *IEEE Transactions on Geoscience and Remote Sensing*, vol. 52, no. 1, pp. 508–518, Jan. 2014, doi: 10.1109/TGRS.2013.2241775.

[21] Z. Zhao, H. Wen, L. Wu, R. Li, T. Zhuang, and Y. Zhang, "Non-Precipitation Echo Identification in X-Band Dual-Polarization Weather Radar," *Remote Sensing*, vol. 17, no. 17, p. 3023, Aug. 2025, doi: 10.3390/rs17173023.

[22] M.-H. Golbon-Haghighi, G. Zhang, Y. Li, and R. Doviak, "Detection of Ground Clutter from Weather Radar Using a Dual-Polarization and Dual-Scan Method," *Atmosphere*, vol. 7, no. 6, p. 83, Jun. 2016, doi: 10.3390/atmos7060083.

[23] J. Yin, H. Chen, Y. Li, and X. Wang, "Clutter Mitigation Based on Spectral Depolarization Ratio for Dual-Polarization Weather Radars," *IEEE Journal of Selected Topics in Applied Earth Observations and Remote Sensing*, vol. 14, pp. 6131–6145, 2021, doi: 10.1109/JSTARS.2021.3088324.

[24] M. Grecu, G. M. Heymsfield, S. Nicholls, S. Lang, and W. S. Olson, "A Machine Learning Approach to Mitigate Ground Clutter Effects in the GPM Combined Radar–Radiometer Algorithm (CORRA) Precipitation Estimates," *Journal of Atmospheric and Oceanic Technology*, vol. 42, no. 1, pp. 17–31, Jan. 2024, doi: 10.1175/JTECH-D-24-0048.1.

[25] R. B. Da Silveira and A. R. Holt, "An automatic identification of clutter and anomalous propagation in polarization-diversity weather radar data using neural networks," *IEEE Transactions on Geoscience and Remote Sensing*, vol. 39, no. 8, pp. 1777–1788, 2001, doi: 10.1109/36.942556.

[26] J. Wang, H. Zou, L. Zhong, and Z. Hu, "Recognition of Ground Clutter in Single-Polarization Radar Based on Gated Recurrent Unit," *Remote Sensing*, vol. 16, no. 23, p. 4609, Dec. 2024, doi: 10.3390/rs16234609.

[27] T. Mäkinen, J. Ritvanen, S. Pulkkinen, N. Weisshaupt, and J. Koistinen, "Bayesian Classification of Nonmeteorological Targets in Polarimetric Doppler Radar Measurements," *Journal of Atmospheric and Oceanic Technology*, vol. 39, no. 10, pp. 1561–1578, Oct. 2022, doi: 10.1175/JTECH-D-21-0177.1

[28] M.-H. Golbon-Haghighi and G. Zhang, "Detection of Ground Clutter for Dual-Polarization Weather Radar Using a Novel 3D Discriminant Function," *Journal of Atmospheric and Oceanic Technology*, vol. 36, no. 7, pp. 1285–1296, Jul. 2019, doi: 10.1175/JTECH-D-18-0147.1.

[29] M. Weber *et al.*, "Towards the Next Generation Operational Meteorological Radar," *Bulletin of the American Meteorological Society*, vol. 102, no. 7, pp. E1357–E1383, Jul. 2021, doi: 10.1175/BAMS-D-20-0067.1.